Desalination and Water Treatment 317 (2024) 100181

Contents lists available at ScienceDirect

Desalination and Water Treatment

journal homepage: www.sciencedirect.com/journal/desalination-and-water-treatment/

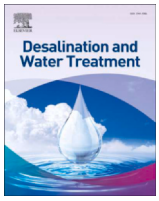

Removal of eutrophication agents from wastewater using glauconite-based sorbents

Kateryna Stepova[a], Iryna Fediv[a,*], Aušra Mažeikienė[b], Vasyl Kordan[c], Dainius Paliulis[b]

[a] Department of Environmental Safety, Lviv State University of Life Safety, 35 Kleparivska str., 79000 Lviv, Ukraine
[b] Department of Environmental Protection and Water Engineering, Faculty of Environmental Engineering, Vilnius Gediminas Technical University, Saulėtekio al. 11, Vilnius 10223, Lithuania
[c] Department of Inorganic Chemistry, Ivan Franko National University of Lviv, Kyryla i Mefodiya St. 6, 79005 Lviv, Ukraine

ARTICLE INFO

Keywords:
Glauconite
Adsorption
Eutrophication agents
Water pollution
Thermal treatment
Microwave irradiation

ABSTRACT

Excessive phosphorus and nitrogen in water and sediment may cause eutrophication, which poses a potential risk to drinking water safety and the sustainability of aquatic ecosystems. The research focuses on the removal of phosphates and ammonium ions from aqueous solutions using a new thermally and microwave-treated glauconite. The surface morphology of the samples was studied by SEM. BET surface area, pore volume, and pore size distribution were measured. Adsorption studies were carried out in static and dynamic conditions. The best fit for adsorption of both pollutants is given by the Langmuir-Freundlich and BET models. The calcined sample showed the lowest adsorption capacity for phosphate (1.78 mg/g) but the highest capacity for ammonium (20.67 mg/g). For the microwave-irradiated sample, the adsorption capacity for ammonium increases from 0.723 to 4.37 mg/g, while that for phosphate remains almost at the same level (101.21 mg/g). In dynamic conditions, phosphorus was most efficiently retained by natural glauconite (more than 60% retention rate), and ammonium nitrogen by glauconite that was thermally treated in a muffle furnace (more than 80% retention rate after 3 h).

1. Introduction

Water pollution is one of the main environmental issues that has released contaminating substances into freshwater bodies or groundwater [1]. Natural water sources are polluted by untreated or insufficiently treated wastewater [2]. A variety of methods and technologies are developed for wastewater treatment. Usually, wastewater is treated using activated sludge microorganisms or chemical reagents. Conventional methods effectively remove organic matter from wastewater, but it is not possible to remove phosphorus completely [3]. Nitrogen is another threatening biogenic element that escapes into the environment with wastewater [4]. In recent years, there has been a significant focus on the advancement of new technologies for environmental protection [5–8]. Excessive P and N in water and sediment can cause eutrophication, which poses a potential risk to drinking water safety and the sustainability of aquatic ecosystems [5]. Effective removal of phosphorus and nitrogen from wastewater is therefore a key strategy to control eutrophication. The final stage of technological processes should be additional treatment with sorbent materials [9]. Adsorption is the most widely used technology for wastewater treatment [6,10–13]. The simplicity of design, speed, efficiency, and profitability determine the wide use of sorbents [14]. Commercially available sorbents are rather expensive, which significantly limits the range of their application areas [15]. In this context, natural clay mineral adsorbents can be used as an alternative [14]. Natural adsorbents are inexpensive, environmentally friendly, and available in large quantities [7,13]. Natural silicates possessing high adsorption, ion exchange, and catalytic characteristics deserve special attention [15–18]. Often, nitrogen in wastewater is in the ammonium form, so it can be removed by ion exchange. Ammonium ions are effectively removed from water or wastewater by zeolites [19,20]. Most clay minerals produce a net negative surface charge due to the isomorphic substitutions of Si (IV) by Al (III) or Fe (III) [1]. Iron-based materials exhibit high efficiency for P immobilization due to their strong affinity with P [5]. The Fe-rich sorbents can effectively immobilize P in sediment under oxic conditions through adsorption and/or precipitation [8,21]. However, not all natural clays are suitable for wastewater treatment. Bauxite and olivine are not applicable due to the presence of significant amounts of lead and/or nickel [22]. Natural sorbents, which include glauconite, are of great interest for wastewater treatment. It can

* Corresponding author.
E-mail address: ira.arnaut94@gmail.com (I. Fediv).

https://doi.org/10.1016/j.dwt.2024.100181
Received 3 February 2024; Received in revised form 3 February 2024; Accepted 7 February 2024

primarily be used as a long-term organic fertilizer because the potassium, iron, and phosphorus present in glauconite pass into the soil and improve its properties [23]. The high efficiency of glauconite has been demonstrated in water purification from heavy metal salts, some organic and inorganic structures, and radionuclides [18,24]. Galangashi et al. used glauconite to remove ammonium ions from water and found that ion exchange was the main mechanism for ammonium removal [25]. The efficiency of sorption in the mineral rock of different deposits is largely determined by the content of granular glauconite in it, as well as the presence of iron oxide in its composition [15]. The advantages of this mineral include widespread distribution, low cost, high availability, grain structure, heat resistance, good ion exchange and filtration properties. [5]. Due to these properties, glauconite can be used in environmental technologies [26,27]. Glauconite is a natural alumosilicate, dioctahedral micaceous phyllosilicate mineral. It is an aqueous aluminosilicate of iron, silica, and potassium oxide with an unstable composition. The final composition may vary depending on the origin of the mineral and affect its sorption properties [5,15]. Clay minerals are considered the most efficient adsorbents, but modification techniques may improve the capacity, ability, and selectivity of clay adsorption properties [1]. Modification processes such as acid activation, heat treatment, column and organic functionalization are used to obtain the desired properties [28–30]. Microwave irradiation has proven to be successful in the preparation of new promising materials for water treatment, causing structural and textural changes that enhance their adsorption capacity [9,31]. The sorption capacity is an important parameter for estimating the lifetime of a sorption material. It is determined during mixing tests. However, a single method for determining the sorption capacity has not yet been developed. For this reason, researchers obtain different values for the sorption capacity of the same materials. On the other hand, only a few studies have focused on actual wastewater treatment.

This research focuses on the removal of phosphates and ammonium ions from aqueous solutions using a new thermally and microwave-treated glauconite. A new method of glauconite modification was proposed, samples modified in several ways were produced and tested, and their properties were compared with the properties of natural glauconite. This work aimed to identify the physicochemical characteristics of Ukrainian glauconite and assess its sorption properties for extracting ammonium ions and phosphates from wastewater.

2. Materials and methods

2.1. Characterization of adsorbents

According to the related literature [32–34], heat treatment of sorbents can harden the structure and increase their sorption capacity. The initial sample of glauconite (pH of aqueous extract – 8.6; bulk density – 1049,85 kg/m3) was sieved to obtain a particle size fraction of 0.8–1.2 mm. To improve the performance characteristics of glauconite, it was pre-treated with the following methods: calcination at 550 ˚C for 3 h, and microwave treatment for 30 min at 790 W.

2.1.1. SEM and EDS

The surface morphology of the powdered samples was studied by scanning electron microscopy (SEM). The qualitative and quantitative composition of the samples was determined using energy dispersive X-ray spectroscopy (EDS) on a Tescan Vega3 LMU electron microscope equipped with the advanced Oxford Instruments Aztec ONE system (CCD Si drift detector X-MaxN20). Before the study, the sample powders were applied to an electrically conductive film. The experiments were performed at a W-cathode voltage of 20–25 kV. The SE detector characterizes the surface morphology and details its irregularities, while the BSE detector shows the contrast of phases with different element fillings.

2.1.2. BET surface area and pore size distribution

Before starting the measurement, the samples were placed in a vacuum and degassed at 150 ˚C for 3 h. BET surface area, pore volume, and pore size distribution of the studied sorbents, as well as nitrogen adsorption/desorption isotherms, were recorded by Quantachrome Autosorb-iQ-KR/MP automated, high-vacuum, gas sorption analyser. Measurements of nitrogen adsorption and desorption isotherms were conducted at − 196 ˚C (77 K). The specific surface area was calculated by the BET (Brunauer–Emmett–Teller) equation. The density functional theory (DFT) and QSDFT method were applied to making the pore size distribution plot. The total pore volume was determined from the adsorption isotherm by measuring the amount of nitrogen adsorbed at a relative pressure of p/p0 = 0.99. All calculations were performed using the ASiQwin program (Version 2.0), developed by Quantachrome Instrument.

2.2. Experiments methodology

2.2.1. Adsorption isotherms

The sorption properties of the samples were investigated under static conditions. Batch experiments were conducted at room temperature for 24 h.

Anhydrous salts KH_2PO_4 and NH_4Cl were used for preparing the model PO_4^{3-} and NH_4^+ solutions respectively. The working solutions were prepared from the initial solutions by repeated dilution with distilled water. The PO_4^{3-} concentration was determined by colorimetric method with Vanadate-molybdate reagent (a mixture of ammonium molybdate and ammonium metavanadate in HNO_3). The photoelectric colorimeter “KFK-2″ was used. Measurement of NH_4^+ content was carried out via the potentiometric method using a “AI-125″ ionomer (DYLYS Ltd., Ukraine) with the accuracy of EMF = ± 0.5 mV. An NH_4-electrode (ELIS-121 NH4, Belarus) was used as an electrode.

The experimental results were fitted to the following three isotherm models:

- the Langmuir-Freundlich isotherm model [35]:

$$q_e = \frac{q_m (K_{LF} C_e)^{n_{LF}}}{1 + (K_{LF} C_e)^{n_{LF}}} \quad (1)$$

where q_e and C_e are and the equilibrium concentrations in solid and liquid phases, respectively. q_m is the adsorption capacity. K_{LF} is the affinity constant, and n_{LF} is the coefficient of heterogeneity or a measure of the adsorption intensity.

- the Dubinin-Radushkevich model [36]:

$$q_e = q_m \exp^{-Be^2} \quad (2)$$

where B is the model's constant, and e – Polanyi potential.

- the BET model [37]:

$$q_e = \frac{q_m C_{BET} C_e}{(C_e - C_S)\left[1 + (C_{BET} - 1)\frac{C_e}{C_S}\right]} \quad (3)$$

where C_{BET} is and constant of the model, and C_S is the concentration of solute at the moment of saturation of all layers.

The nonlinear modeling was carried out according to the procedure described in our previous works [38].

2.2.2. Breakthrough curves

The chemical laboratory of VILNIUS TECH was equipped with three-column stand (Fig. 1).

The stand was made of three transparent glass columns with valves and hoses for leachate drainage at the bottom. Domestic wastewater (which had already been biologically treated in an individual unit) was filtered on the laboratory stand. COD, BOD and TSS in the biologically (using activated sludge) treated wastewater were 45 mgO_2/L, 8 mgO_2/L

Fig. 1. Laboratory bench with three columns.

and 5 mgO_2/L, respectively. The pH value of the treated wastewater was 7.5. The initial concentration of PO_4-P in the wastewater was 4.85 mg/L, and the initial concentration of NH_4-N was 16.1 mg/L. The wastewater was transferred from the container into a beaker and poured into the columns, maintaining the same height (15 cm) of the liquid layer. By opening the valves at the bottom of the columns, the constant filtration rate (5 ml/min) was regulated. During the filtration, the fillers of all three columns were submerged and a layer of liquid 10–15 cm high was maintained above them. The three columns were filled as follows (Table 1):

Glauconite powder (fraction 0.005 mm) was mixed with quartz sand so that it would not stick together into a single mass for filtration. The filtration experiment lasted 4 h. Filtrate samples were taken hourly for ammonium nitrogen and phosphate phosphorus concentration. The experiment was repeated 3 times, and the figures show the average values.

The effectiveness of removing PO_4-P from wastewater was calculated according to formula (4):

$$E_i = \frac{(C_{1i} - C_{2i})}{C_{1i}} \cdot 100 \quad (4)$$

where: E_i – effectiveness of PO_4-P removing, %; $C_{1,i}$ – concentration of PO_4-P before treatment, mg/L; $C_{2,i}$ – concentration of PO_4-P after treatment, mg/L. The study was repeated to present the mean results of three experiments.

MERCK Spectroquant® tests were used to determine the phosphorus concentration of phosphates. Test limits 0.50–30.0 mg/l PO_4-P. Absorbance measurements of the test solution were performed by pouring test samples into 10 mm cuvettes (Hellma) and measuring at the required wavelength (410 nm) with a Genesys 10 UV–Vis spectrophotometer (Thermo Fisher Scientific, USA). MERCK Spectroquant® tests were used to determine ammonium nitrogen concentration. Test limits 2.0–75.0 mg/l NH_4-N. Absorbance measurements of the test solution were performed after 15 min by pouring test samples into 10 mm cuvettes (Hellma) and measuring at the required wavelength (690 nm) with a Genesys 10 UV–Vis spectrophotometer (Thermo Fisher Scientific, USA).

3. Results and discussion

3.1. SEM and EDS

Fig. 2 shows the surface morphology of powdered samples of natural glauconite. The size of the crystallites of the original sample is 2–20 μm. The shape of the grains is similar to blocks with cut edges. The peculiarity of the stacking of these blocks is significant aggregation between them, probably due to crystallization water.

Heat or microwave treatment changes both the grain shape and morphology of the sample. Large aggregates of ~20 μm crack into smaller fragments (5–10 μm) with a highly developed surface during processing. In the case of thermal treatment, spherical particles can be observed next to the blocky grains. On the surface of each particle, we can see microcracks, which contribute to further amorphization of the sample as the processing time increases. A similar effect is observed for the sample after microwave treatment. The evaporation of crystallization water causes the formation of micropores and microcracks and increases the surface area of the grains for further sorption of ammonium (NH_4^+) and phosphate (PO_4^{3-}) ions.

The overall composition of the sample does not undergo significant changes, as water is mainly released during the treatment. Some changes are due to the heterogeneity of the composition of natural glauconite. Fig. 3 shows the elemental distribution on the sample surface. The ratio of cations for the original sample is Na/Mg/Al/Si/K/Ca/Ti/Fe 1.17/1.07/13.39/74.41/4.45/4.00/0.35/1.16. The elemental ratios for the muffle furnace-annealed and microwave-irradiated samples are Mg/Al/Si/K/Ca/Fe 5.20/11.35/59.90/7.82/3.30/12.43 and Mg/Al/Si/K/Ca/Fe 5.76/11.52/58.36/7.42/4.09/12.85, respectively.

3.2. Surface area and porosity

The N_2 adsorption-desorption isotherms for natural and modified samples are presented in Fig. 4. Due to hysteresis loops present on the

Table 1
Column fillers.

Layer height (cm)	Column 1	Column 2	Column 3
3	supporting layer of pebbles	supporting layer of pebbles	supporting layer of pebbles
7	layer of quartz sand	layer of quartz sand	layer of quartz sand
4	mixed filler: glauconite (3 h in a muffle furnace at a temperature of 550 °C) plus 60 g of quartz sand	mixed filler: natural glauconite plus 60 g of quartz sand	mixed filler: glauconite (30 min under the influence of microwaves) plus 60 g of quartz sand
1.5	20 g of quartz sand	20 g of quartz sand	20 g of quartz sand

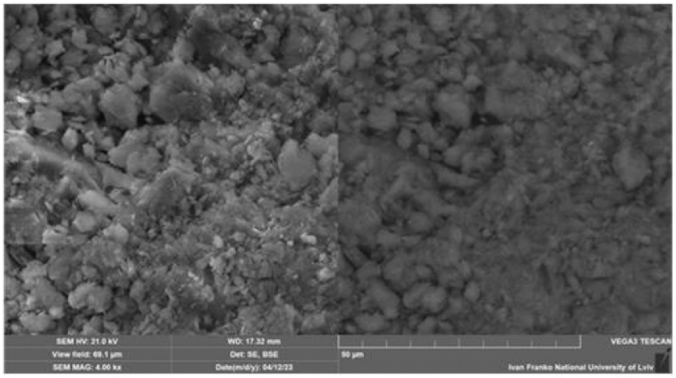

a

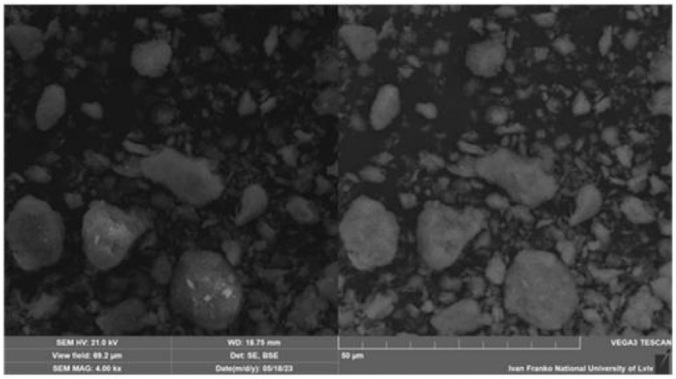

b

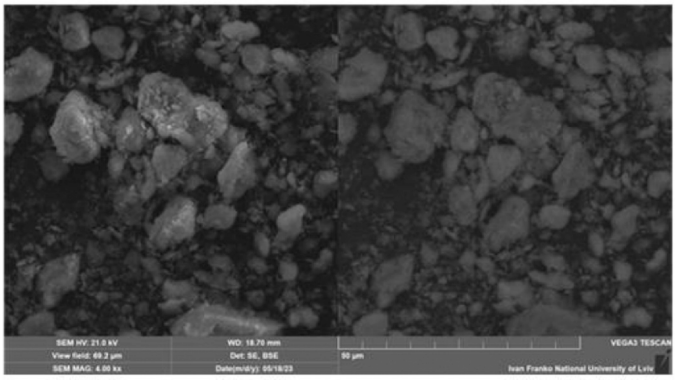

c

Fig. 2. SEM images of glauconite (SE detector on the left, BSE detector on the right): a - initial sample, b - calcined at 550 °C, c - microwave irradiated.

plot of the samples we assume that the materials are mesoporous. The hysteresis loops in all the isotherms are of type IV (IUPAC) with the loops of the H3 type [39]. The H3 type is characterized by the presence of wedge-shaped pores, resulting from the loose arrangement of flaky particles. It is evident on the micrographs of the test samples (Fig. 4).

The results of porosimetry are presented in Table 2. The equivalent particle size (d_{part}) was estimated using the relation (5) [40]:

$$d_{part} = \frac{6000}{S_{BET} \bullet \rho} \tag{5}$$

where ρ is the density of bulk composite in g/cm^3 and S_{BET} is expressed in m^2/g. The porosity of the particles (ε) is calculated using the following Eq. (6) [41]:

$$\varepsilon = \frac{V_p}{V_p + 1/\rho_{app}} \tag{6}$$

where Vp is the pore volume (cm^3/g) and ρ_{app} is the apparent density (g/cm^3) of investigated materials.

It was found that high-temperature treatment reduces the BET surface area from 54.99 to 43.57 m^2/g. In contrast, under the influence of microwave irradiation, the surface area changes much less. However, an interesting fact was the increase in the external surface area of the glauconite sample under the influence of microwave irradiation with a simultaneous decrease in the micropore area. Whereas calcination at 550 °C causes only a decrease in the micropore surface area (Fig. 5). Expectedly, the equivalent particle size increases under the influence of high temperature due to sintering from 103.9 to 156.7 nm.

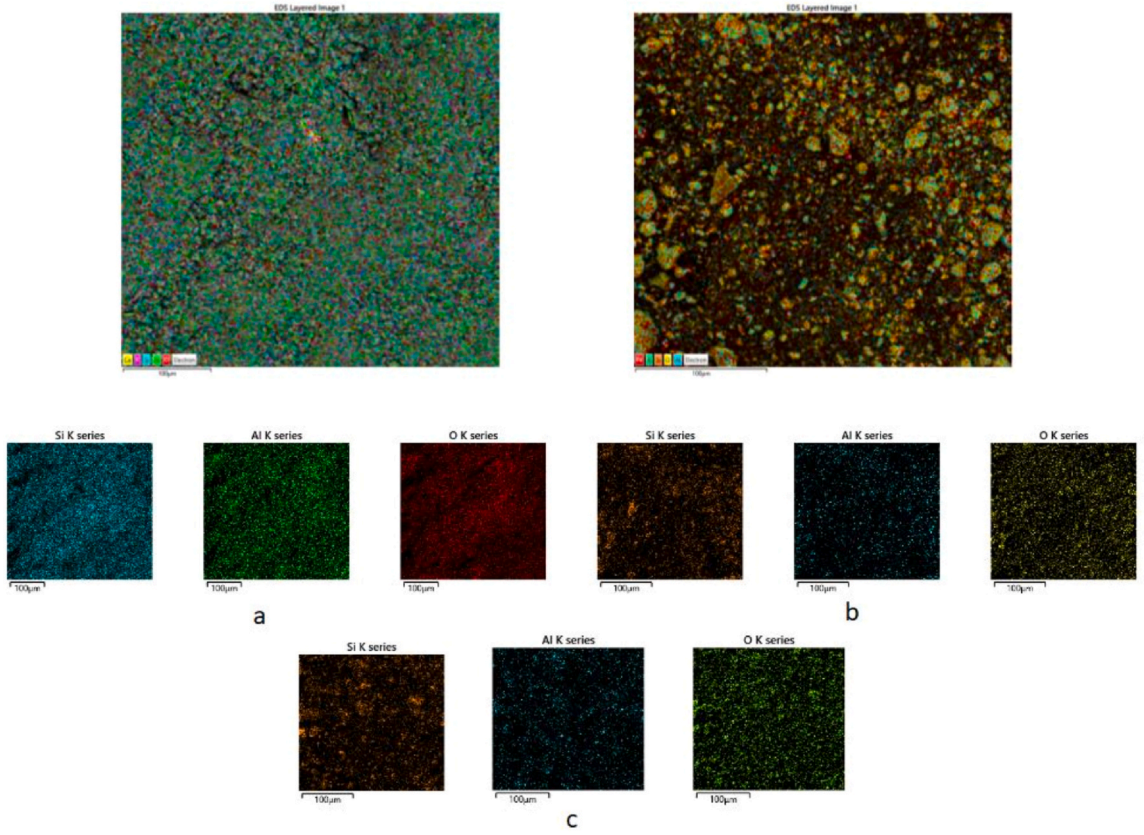

Fig. 3. Elemental distribution on the surface of glauconite. a - initial sample, b - calcined at 550 °C, c - microwave irradiated.

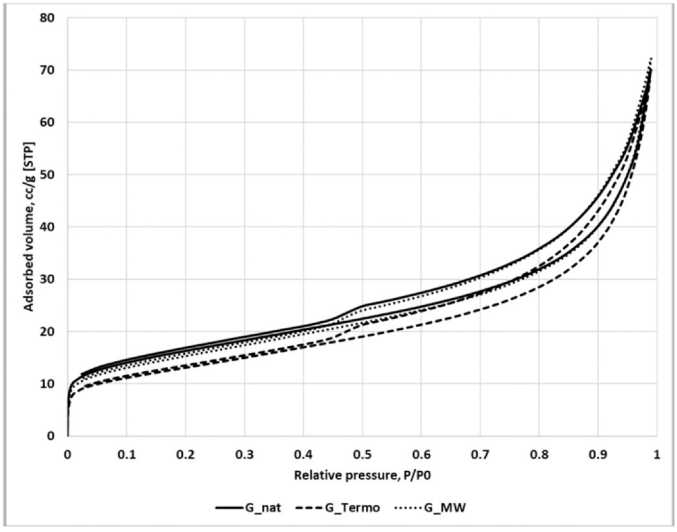

Fig. 4. N_2 adsorption-desorption isotherms.

Table 2
Specific surface area (S_{BET}), micropore area (S_{mic}), external surface area (S_{ext}), pore volume (V_p), equivalent particle size (d_{part}), and porosity (ε) of natural and modified clinoptilolite.

Sample code	S_{BET}, m^2/g	S_{mic}	S_{ext}	V_p, ml/g	d_{part}, nm	ε
G_nat	54.99	26.0	28.99	0.084	103.9	0.081
G_thermo	43.57	14.9	28.67	0.083	156,7	0.068
G_MW	50.28	20.1	30.18	0.086	107.3	0.087

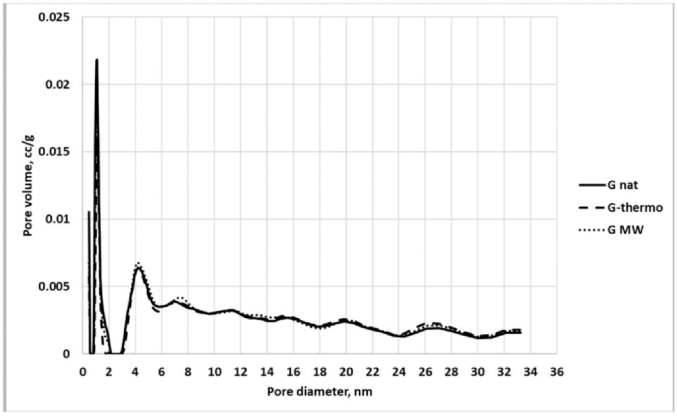

Fig. 5. Pore size distribution.

Table 3
NH_4^+ adsorption isotherms nonlinear fitting parameters.

	Sample index		
	G_nat	G_thermo	G_MW
Langmuir-Feundlich isotherm			
q_m	0.723	20.67	4.37
K_{FL}	0.025	0.0018	0.0015
n_{FL}	2.503	1.027	0.96
SNE	3.65	4.1	3.54
R^2	1.0	1.0	1.0
Dubinin-Radushkevich isotherm			
q_m	4.286	4.695	1.052
β	0.041	0.021	0.021
SNE	23.03	26.01	23.64
R^2	0.97	0.97	0.94
BET isotherm			
q_m	0.0012	236.29	115.95
C_{BET}	1.07	0.28	0.84
SNE	6.20	5.68	4.85
R^2	0.93	0.99	0.97

Table 4
PO_4^{3-} adsorption isotherms nonlinear fitting parameters.

	Sample index		
	G_nat	G_thermo	G_MW
Langmuir-Feundlich isotherm			
q_m	113.58	1.78	101.21
K_{FL}	0.0062	0.0186	0.0055
n_{FL}	3.275	8.352	2.77
SNE	3.52	3.64	3.83
R^2	1.0	1.0	1.0
Dubinin-Radushkevich isotherm			
q_m	140	212.07	194.2
β	0.075	0.24	0.078
SNE	198.4	129.1	61.74
R^2	0.95	0.92	0.93
BET isotherm			
q_m	100.15	100.18	100.04
C_{BET}	0.01	0.0012	0.02
SNE	7.97	6.89	4.81
R^2	0.99	1.0	0.98

3.3. Adsorption isotherms

According to Xu et al. (2018) the microwave activation increases the adsorbent surface area, micropore volume and total pore volume, which can improve the adsorption capacity. Microwave modification can achieve uniform and rapid heating, and create new or unique pore structures. However, part of the chemisorption sites on adsorbent surface may be removed after microwave activation, resulting in the decrease of adsorption capacity. Therefore, microwave activation serves as an auxiliary method to improve the surface structure of adsorbents [42]. In [43] Langmuir, Temkin, Freundlich and Dubinin–Radushkevich isoterms were tested for description of experimental data. NH_4^+ adsorption onto the glauconite was well described by Freundlich an Langmuir isotherm models. In our work we've chosen three-parameter Lengmuir-Feundich and BET models for better fit, and Dubinin-Radushkevich isotherm as it can be used to determine the nature of adsorption. The results of the nonlinear fitting of experimental research within theoretical models are presented in Tables 3 and 4.

All three models demonstrate rather good fit, though the best fit for adsorption of the both pollutants is given by Langmuir-Freundlich model. It gives and opportunity to compare the maximum adsorption capacity of the samples, but it doesn't provide any information about the adsorption mechanism. In order to define the physical or chemical mechanism of adsorption the Dubinin-Radushkevich isotherm was used. From the determination of the average free energy of adsorption (E), the nature of the process can be inferred. The calculated values of E in all studied cases are less than 8 kJ/mol, so the adsorption process is of physical nature [44]. Meanwhile the BET model also fits well to experimental data. This model describes the physical adsorption process rather well and allows the formation of n layers. So, as the R^2 value tends to unity, it may be assumed that the polymolecular layer is formed in the pores of the investigated samples, indicating that physical adsorption prevails. The adsorption isotherms of NH_4^+ and PO_4^{3-} on natural and modified clinoptilolite are presented in Figs. 6 and 7 respectively.

The shapes of the curves are quite different. The isotherm of NH_4^+ adsorption corresponds to Type-IV according to the IUPAC classification [45], while the PO_4^{3-} isotherm corresponds to the Type-V. According to [46], Type-V isotherms are related to microporous materials, as opposed to the Type-VI isotherm where multilayer adsorption occurs on a uniform non-porous surface [47]. Therefore, it can be assumed that NH_4^+ is absorbed by the external surface of the samples, but phosphate ion is well fixed in the micropores. This coincides with the results of the porosity study of the samples before and after treatment. As shown in Table 2, heat treatment at high temperatures leads to a significant decrease in microporosity by 42.3%. Therefore, it is the calcined sample that shows the lowest adsorption capacity for phosphate of 1.78 mg/g (according to Langmuir-Freundlich model). In contrast, this increases the adsorption capacity of the sample for ammonium from 0.723 to 20.67 mg/g. Besides, for the microwave-irradiated sample, the adsorption capacity for ammonium increases from 0.723 to 4.37 mg/g, while that for phosphate remains almost at the same level (101.21 mg/g).

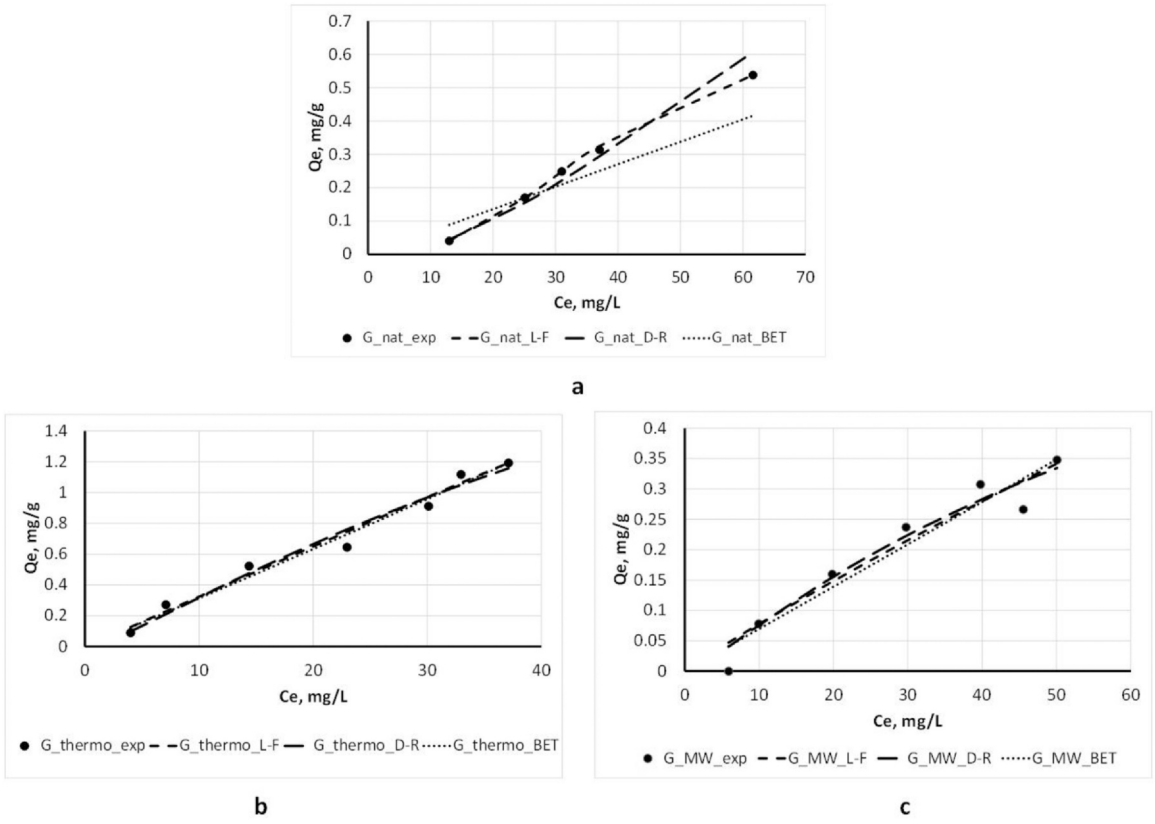

Fig. 6. Isotherms of NH_4^+ adsorption: a - initial sample, b - calcined at 550 °C, c - microwave irradiated.

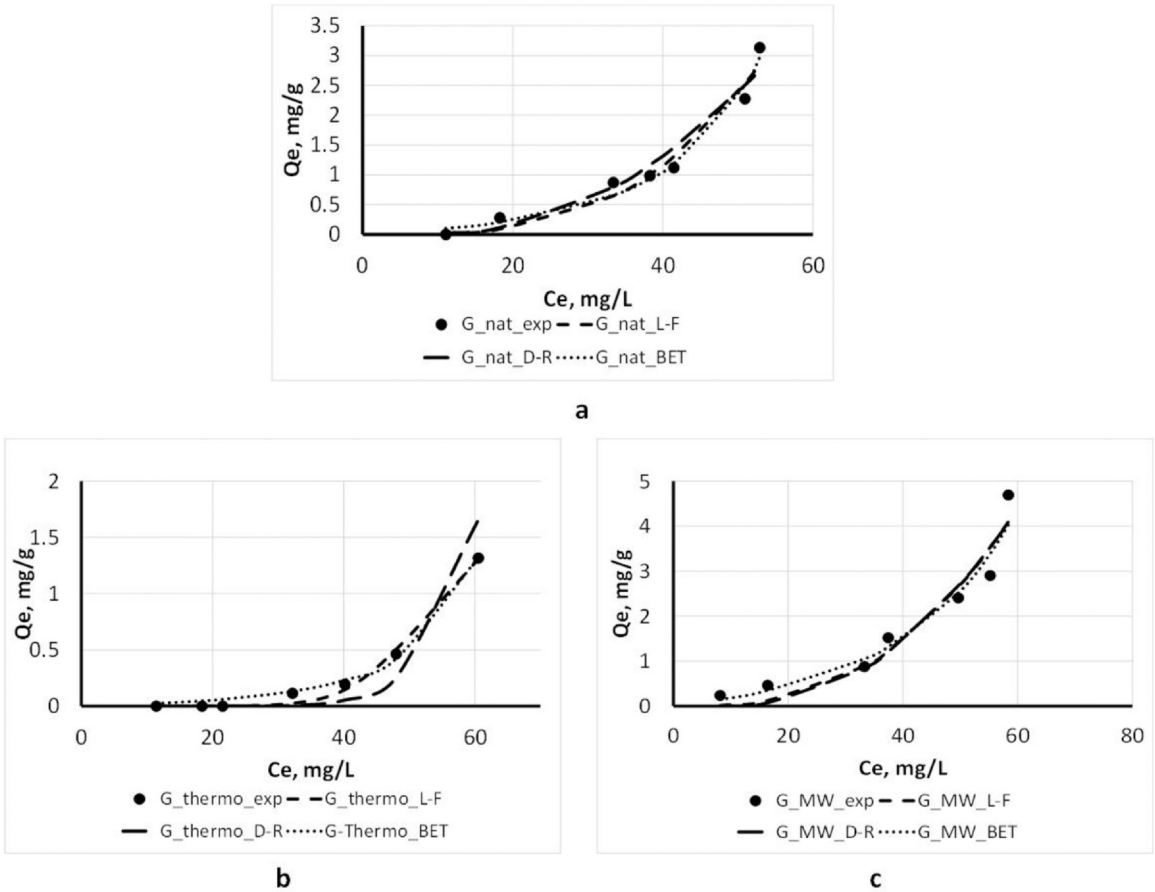

Fig. 7. Isotherms of PO_4^{3-} adsorption: a - initial sample, b - calcined at 550 °C, c - microwave irradiated.

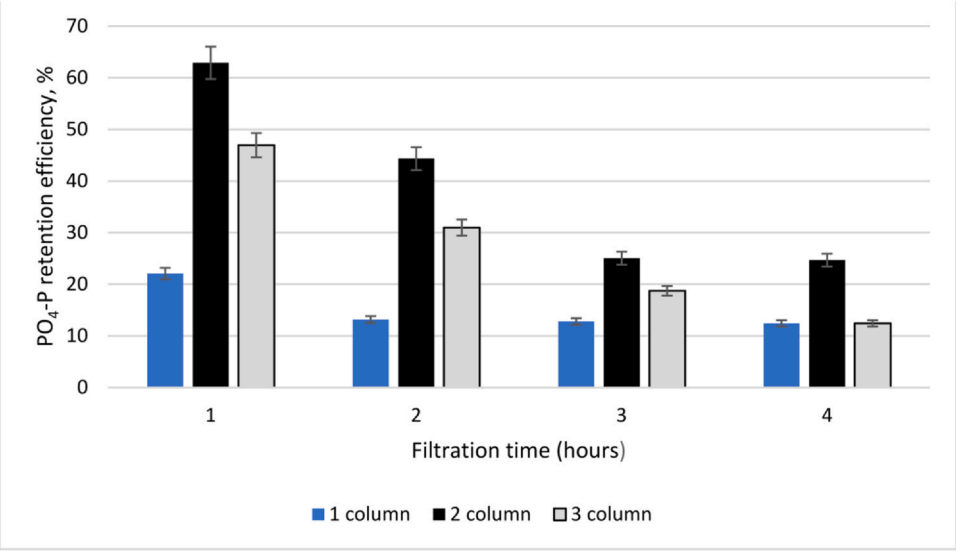

Fig. 8. PO_4-P retention efficiency.

3.4. Breakthrough capacity

Gauconite is a silicate class mineral containing Na, Mg, Al, Si, K, Ca, Fe cations. It has been observed that ion exchange dominates ammonium adsorption when using aluminosilicate materials. Ammonium forms in solution are affected by pH and temperature. At pH < 7, more than 95% of ammonium is in the ionized form (NH_4^+), which promotes ion exchange [48]. In this work, the filtration test was performed on biologically treated wastewater with a pH of 7.5. The sorption capacity of NH_4^+ onto the glauconite was found to be comparable and moderately higher than that of many other corresponding sorbents reported in the literature. The adsorption capacity of NH_4^+ onto the glauconite was 19.24 mg/g, when pH = 7 and initial concentration was 10 mg/L [48].

Based on experimental studies conducted by Berkessa et al. (2019), it was determined that the optimal pH value for phosphate adsorption is 7. During adsorption, chemical sorption dominated [49]. Authors Abukharda et al. (2020), using a synthesized bentonite/zeolite–P (BE/ZP) composite, achieved the best results for phosphate and ammonium removal from wastewater at pH = 6, efficiency 62% and 75% respectively [50].

Fig. 8 clearly demonstrates that, in the initial two hours, both the natural and microwave-irradiated samples exhibited the highest effectiveness of PO_4^{3-} removal compared to the thermally treated sorbent. Three hours later, all the samples reached almost the same retention rate. The best result in terms of phosphate uptake was shown by the natural glauconite and slightly worse by the microwave irradiated sample. Thermal modification significantly worsens the sorption properties of glauconite for phosphate. Thus, in the case of phosphate absorption under dynamic conditions, heat treatment of glauconite does not lead to a significant improvement in sorption properties.

A completely opposite phenomenon is observed in the ammonium absorption. As can be seen from Fig. 9, the highest removal rate during the first hour is demonstrated by the natural and heat-treated samples. However, subsequently, the ammonium retention efficiency begins to decrease sharply for both the natural and microwave irradiated samples. At the same time, the heat-treated sorbent continues to effectively purify water (more than 80% efficiency) even after 3 h of exposure. Thus, in the case of ammonium nitrogen purification, heat treatment of glauconite significantly improves its sorption capacity.

Hence, phosphate phosphorus and ammonium nitrogen retention took place in all the columns. Phosphorus was most efficiently retained by natural glauconite, and ammonium nitrogen by glauconite that was calcinated in a muffle furnace for 3 h at 550 °C. In general, all three columns removed ammonium nitrogen more efficiently than phosphate phosphorus.

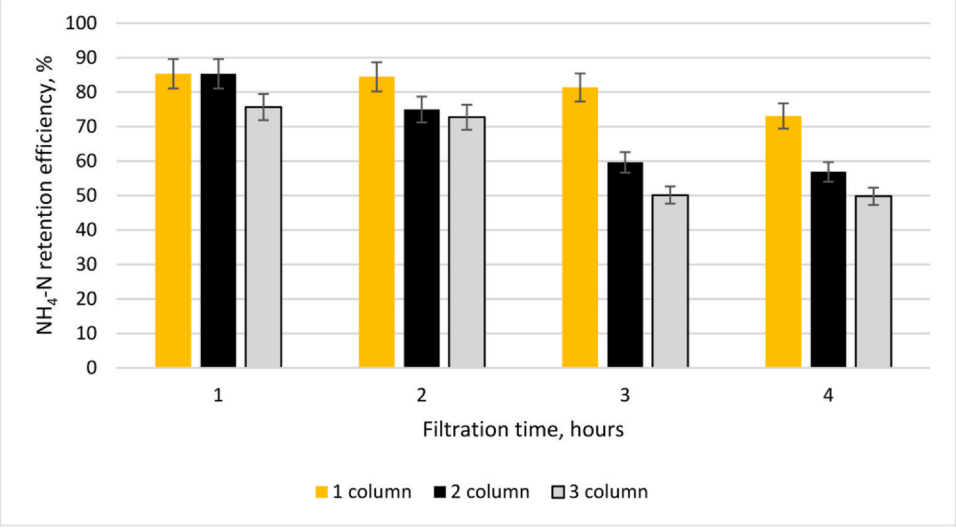

Fig. 9. NH_4-N retention efficiency.

4. Conclusions

New thermally and microwave-treated glauconite for removal of eutrophication agents (phosphate phosphorus and ammonium nitrogen) from aqueous solutions was investigated.

SEM-EDS investigation revealed that heat or microwave treatment changes both the grain shape and morphology of the sample. Large aggregates of ~20 μm crack into smaller fragments (5–10 μm) with a highly developed surface during processing. The evaporation of crystallization water causes the formation of micropores and microcracks and increases the surface area of the grains for further sorption of ammonium (NH_4^+) and phosphate (PO_4^{3-}) ions. Heat and microwave treatment of glauconite causes similar changes in the cation ratio.

Measurements of the BET surface area showed that high-temperature treatment leads to its reduction. However, it is important to note that this decrease is primarily attributed to the reduction in micropore surface area. Whereas the increase in the external surface area of the glauconite sample under the influence of microwave irradiation is accompanied by a decrease in the micropore area.

The best fit for the adsorption isotherm of both pollutants is given by Langmuir-Freundlich and BET models. The values of average free energy calculated from Dubinin-Radushkevich model were less than 8 kJ/mol, so the adsorption process is of a physical nature. The shapes of the phosphate and ammonia adsorption isotherms are quite different. The shape of PO_4^{3-} isotherm is of the type related to microporous materials, as opposed to the type of NH_4^+ isotherm where multilayer adsorption occurs on a uniform non-porous surface. Therefore, it can be assumed that NH_4^+ is absorbed by the external surface of the samples, but phosphate ion is well fixed in the micropores. This coincides with the results of the porosity study of the samples before and after treatment. Moreover, it is the calcined sample that shows the lowest adsorption capacity for phosphate but the better adsorption capacity for ammonium. Conversely, for the microwave-irradiated sample, the adsorption capacity for phosphate increases, while that for ammonium remains at the same level.

The best result in phosphate uptake in dynamic conditions was shown by the natural glauconite and slightly worse by the microwave-irradiated sample. Thermal modification significantly worsens the sorption properties of glauconite for phosphate. A completely opposite phenomenon is observed in the ammonium absorption. The highest removal rate during the first hour is demonstrated by the natural and heat-treated samples. However, subsequently, the ammonium retention efficiency begins to decrease sharply for both the natural and microwave-irradiated samples. At the same time, the heat-treated sorbent continues to effectively purify water (more than 80% efficiency) even after 3 h of exposure. Thus, in the case of ammonium nitrogen purification, heat treatment of glauconite significantly improves its sorption capacity. In general, all three columns removed ammonium nitrogen more efficiently than phosphate phosphorus.

Author contributions

Conceptualization, K.S, I.F, A.M. and V.K.; Methodology, K.S., A.M., V.K and D.P.; Validation, K.S., I.F. and D.P.; Formal analysis, K.S., I.F. and A.M.; Investigation, K.S., I.F., A.M., V.K. and D.P.; Resources, K.S., I.F., A.M. and V.K.; Data curation, K.S., A.M. and D.P.; Writing – original draft, K.S., I.F., A.M., V.K. and D.P.; Writing – review & editing, K.S., A.M., and D.P.; Visualization, K.S., I.F., A.M., V.K and D.P.; Supervision, K.S. and A.M. All authors have read and agreed to the published version of the manuscript.

Funding

This research was funded by Research Council of Lithuania and Ministry of Education and Science of Ukraine, according to the project “Sustainable technology of wastewater treatment by environmentally friendly modified natural sorbents for removal of nitrogen, phosphorus and surfactants”, financing agreement No. S-LU-22-1.

Declaration of Competing Interest

The authors declare that they have no known competing financial interests or personal relationships that could have appeared to influence the work reported in this paper.

References

[1] Barakan S, Aghazadeh V. The advantages of clay mineral modification methods for enhancing adsorption efficiency in wastewater treatment: a review. Environ Sci Pollut Res 2021;28:2572–99. https://doi.org/10.1007/s11356-020-10985-9.
[2] Jones ER, Bierkens MFP, Wanders N, et al. Current wastewater treatment targets are insufficient to protect surface water quality. Commun Earth Environ 2022;3:221. https://doi.org/10.1038/s43247-022-00554-y.
[3] Mažeikienė A, Grubliauskas R. Biotechnological wastewater treatment in small-scale wastewater treatment plants. J Clean Prod 2021;279:123750. https://doi.org/10.1016/j.jclepro.2020.123750.
[4] Janicka E, Kanclerz J, Wiatrowska K, Budka A. Variability of nitrogen and phosphorus content and their forms in waters of a river-lake system. Front Environ Sci 2022;10:874754. https://doi.org/10.3389/fenvs.2022.874754.
[5] Wang Q, Liao Z, Yao D, Yang Z, Wu Y, Tang C. Phosphorus immobilization in water and sediment using iron-based materials: a review. Sci Total Environ 2021;767:144246. https://doi.org/10.1016/j.scitotenv.2020.144246.
[6] Ding S, Sun Q, Chen X, Liu Q, Wang D, Lin J, et al. Synergistic adsorption of phosphorus by iron in lanthanum modified bentonite (Phoslock®): new insight into sediment phosphorus immobilization. Water Res 2018;134:32–43. https://doi.org/10.1016/j.watres.2018.01.055.
[7] Han H, Rafiq MK, Zhou T, Xu R, Mašek O, Li X. A critical review of clay-based composites with enhanced adsorption performance for metal and organic pollutants. J Hazard Mater 2019;369:780–96. https://doi.org/10.1016/j.jhazmat.2019.02.003.
[8] Ezzatahmadi N, Ayoko GA, Millar GJ, Speight R, Yan C, Li J, et al. Clay-supported nanoscale zero-valent iron composite materials for the remediation of contaminated aqueous solutions: a review. Chem Eng J 2017;312:336–50.
[9] Stepova K, Fediv I, Mažeikienė A, Šarko J, Mažeika J. Adsorption of ammonium ions and phosphates on natural and modified clinoptilolite: isotherm and breakthrough curve measurements. Water 2023;15:1933. https://doi.org/10.3390/w15101933.
[10] Xia L, David T, Verbeeck M, Bruneel Y, Smolders E. Iron rich glauconite sand as an efficient phosphate immobilising agent in river sediments. Sci Total Environ 2022;811:152483. https://doi.org/10.1016/j.scitotenv.2021.152483.
[11] Vandermoere S, Ralaizafisoloarivony NA, Van Ranst E, De Neve S. Reducing phosphorus (P) losses from drained agricultural fields with iron coated sand (-glauconite) filters. Water Res 2018;141:329–39. https://doi.org/10.1016/j.watres.2018.05.022.
[12] Chauhan M, Saini VK, Suthar S. Enhancement in selective adsorption and removal efficiency of natural clay by intercalation of Zr-pillars into its layered nanostructure. J Clean Prod 2020;258:120686. https://doi.org/10.1016/j.jclepro.2020.120686.
[13] Chang YS, Au PI, Mubarak NM, Khalid M, Jagadish P, Walvekar R, et al. Adsorption of Cu(II) and Ni(II) ions from wastewater onto bentonite and bentonite/GO composite. Environ Sci Pollut Res 2020;27(*26*):33270–96. https://doi.org/10.1007/s11356-020-09423-7.
[14] Turki T, Frini-Srasra N, Srasra E. Environmental Application of Acid Activated Kaolinite-Glauconite Clay Assisted by Microwave Irradiation. Silicon 2022;14:7939–49. https://doi.org/10.1007/s12633-021-01531-4.
[15] Martemyanov D, Rudmin M, Zhuravkov S, Korotkova E, Godymchuk A, Haskelberg M, et al. Application of ural glauconite for groundwater deironing and demanganation. J Environ Sci Health A 2021;56(*8*):861–6. https://doi.org/10.1080/10934529.2021.1932171.
[16] Georgescu A-M, Nardou F, Zichil V, Nistor ID. Adsorption of lead(II) ions from aqueous solutions onto Cr-pillared clays. Appl Clay Sci 2018;152:44–50. https://doi.org/10.1016/j.clay.2017.10.031.
[17] El Ouardi M, Laabd M, Abou Oualid H, Brahmi Y, Abaamrane A, Elouahli A, et al. Efficient removal of p-nitrophenol from water using montmorillonite clay: insights into the adsorption mechanism, process optimization, and regeneration. Environ Sci Pollut Res Int 2019;26(*19*):19615–31. https://doi.org/10.1007/s11356-019-05219-6.
[18] Bruneel Y, Van Laer L, Brassinnes S, Smolders E. Radiocaesium sorption on natural glauconite sands is unexpectedly as strong as on boom clay. Sci Total Environ 2020;720:137392. https://doi.org/10.1016/j.scitotenv.2020.137392.
[19] Pinelli D, Foglia A, Fatone F, Papa E, Maggetti C, Bovina S, et al. Ammonium recovery from municipal wastewater by ion exchange: development and application of a procedure for sorbent selection. J Environ Chem Eng 2022;10(*6*):108829. https://doi.org/10.1016/j.jece.2022.108829.
[20] Guida S, Potter C, Jefferson B, et al. Preparation and evaluation of zeolites for ammonium removal from municipal wastewater through ion exchange process. Sci Rep 2020;10:12426. https://doi.org/10.1038/s41598-020-69348-6.
[21] Mucci M, Maliaka V, Noyma NP, Marinho MM, Lürling M. Assessment of possible solid-phase phosphate sorbents to mitigate eutrophication: influence of pH and anoxia. 1431–1440 Sci Total Environ2018:619–20. https://doi.org/10.1016/j.scitotenv.2017.11.198.

[22] Vandermoere S, Ralaizafisoloarivony NA, Van Ranst E, De Neve S. Reducing phosphorus (P) losses from drained agricultural fields with iron coated sand (-glauconite) filters. Water Res 2018;141:329–39. https://doi.org/10.1016/j.watres.2018.05.022.
[23] Rudmin M, Banerjee S, Makarov B. Evaluation of the effects of the application of glauconitic fertilizer on oat development: a two-year field-based investigation. Agronomy 2020;10:872. https://doi.org/10.3390/agronomy10060872.
[24] Martemianov D, Plotnikov E, Rudmin M, Tyabayev A, Artamonov A, Kundu P. Studying glauconite of the bakchar deposit (Western Siberia) as a prospective sorbent for heavy metals. J Environ Sci Health A 2020;55:1359–65. 10. 1080/10934529.2020.1794686.
[25] Galangashi MA, Kojidi SFM, Pendashteh A, Souraki BA, Mirroshandel AA. Removing iron, manganese and ammonium ions from water using greensand in fluidized bed process. J Water Process Eng 2021;39:101714. https://doi.org/10.1016/j.jwpe.2020.101714.
[26] Singla R, Alex TC, Kumar R. On mechanical activation of glauconite: Physicochemical changes, alterations in cation exchange capacity and mechanisms. Powder Technol 2020;360:337–51. https://doi.org/10.1016/j.powtec.2019.10.035.
[27] Cecilia J, García-Sancho C, Vilarrasa-García E, Jiménez-Jiménez J, Rodriguez-Castellón E. Synthesis, characterization, uses and applications of porous clays heterostructures: a review. Chem Rec 2018;18:1085–104.
[28] Kotova DL, Artamonova MN, Krysanova TA, et al. The effect of a pulsed magnetic field on the hydration properties of clinoptilolite and glauconite. Prot Met Phys Chem Surf 2018;54:598–602. https://doi.org/10.1134/S2070205118030073.
[29] Khabbouchi M, Hosni K, Mezni M, Srasra E. Structural characterizations and mechanical behavior of activated clay-based $Si_5(PO_4)_6O$ and SiP_2O_7 compounds. Silicon 2019;12(*8*):117–24. https://doi.org/10.1007/s12633-019-00218-1.
[30] Cherifi Z, Boukoussa B, Zaoui A, Belbachir M, Meghabar R. Structural, morphological and thermal properties of nanocomposites poly(GMA)/clay prepared by ultrasound and in-situ polymerization. Ultrason Sonochem 2018;48:188–98. https://doi.org/10.1016/j.ultsonch.2018.05.027.
[31] Pozo-Rodríguez M, Pardo-Canales L, Essih S, Cecilia JA, Dominguez-Maqueda M, Olmo-Sanchez MI, et al. Modification of the textural properties of palygorskite through microwave assisted acid treatment. Influence of the octahedral sheet composition. Appl Clay Sci 2020;196:105745. https://doi.org/10.1016/j.micromeso.2019.109749.
[32] Krol M, Rozek P. The effect of calcination temperature on metakaolin structure for the synthesis of zeolites. Clay Min 2018;53:657–63. https://doi.org/10.1180/clm.2018.49.
[33] Zhang A, Liu J, Yang Y, Yu Y, Wu D. Experimental and theoretical studies on the adsorption performance of lead by thermal pre-activation and phosphate modified kaolin sorbent. *Part 2* Chem Eng J 2023;451:138762. https://doi.org/10.1016/j.cej.2022.138762.
[34] Zha J, Huang Y, Clough PT, Xia Z, Zhu Z, Fan C, et al. Green production of a novel sorbent from kaolin for capturing gaseous $PbCl_2$ in a furnace. (Part B). J Hazard Mater 2021;404:124045. https://doi.org/10.1016/j.jhazmat.2020.124045.
[35] Sips R. Combined form of Langmuir and Freundlich equations. J Chem Phys 1948;16:490–5. https://doi.org/10.1063/1.1746922.
[36] Dubinin MM. Physical Adsorption of Gases and Vapors in Micropores. In: Cadenhead DA, Danielli JF, Rosenberg MD, editors. In Progress in Surface and Membrane Science; Volume 9. Elsevier; 1975. p. 1–70. https://doi.org/10.1016/B978-0-12-571809-7.50006-1.
[37] Brunauer S, Emmett PH, Teller E. Adsorption of Gases in multimolecular layers. J Am Chem Soc 1938;60(*2*):309–19.
[38] Stepova K, Sysa L, Konanets R. Nonlinear Fitting of Iron Sorption on Bentonite to Theoretical Isotherm Models. Phys Chem Solid State 2022;23(*2*):270–6. https://doi.org/10.15330/pcss.23.2.270-276.
[39] Zhang SN, Xiao RL, Liu F, Wu JS. Interception effect of vegetated drainage ditch on nitrogen and phosphorus from drainage ditches. Huanjing Kexue/Environ Sci 2015;36:4516–22. https://doi.org/10.13227/j.hjkx.2015.12.025.
[40] Thommes M, Kaneko K, Neimark AV, Olivier JP, Rodriguez-Reinoso F, Rouquerol J, et al. Physisorption of gases, with special reference to the evaluation of surface area and pore size distribution (IUPAC Technical Report). Pure Appl Chem 2015;87:1051–69. https://doi.org/10.1515/pac-2014-1117.
[41] Lambert S, Tran KY, Arrachart G, Noville F, Henrist C, Bied C, et al. Tailor-made morphologies for Pd/SiO_2 catalysts through sol–gel process with various silylated ligands. Microporous Mesoporous Mater 2008;115:609–17. https://doi.org/10.1016/j.micromeso.2008.03.003.
[42] Xu W, Hussain A, Liu Y. A review on modification methods of adsorbents for elemental mercury from flue gas. J Chem Eng 2018;346:692–711. https://doi.org/10.1016/j.cej.2018.03.049.
[43] Naghipour D, Taghavi K, Ashournia M, Jaafari J, Arjmand Movarrekh R. A study of Cr (VI) and NH4 + adsorption using greensand (glauconite) as a low-cost adsorbent from aqueous solutions. Water Environ J 2020;34(1):45–56. https://doi.org/10.1111/wej.12440.
[44] Kundu Sanghamitra, Gupta AK. Arsenic adsorption onto iron oxide-coated cement (IOCC): Regression analysis of equilibrium data with several isotherm models and their optimization. Chem Eng J 2006;122(1–2):93–106. https://doi.org/10.1016/j.cej.2006.06.002.
[45] Thommes M, Kaneko K, Neimark AV, Olivier JP, Rodriguez-Reinoso F, Rouquerol J, et al. Physisorption of gases, with special reference to the evaluation of surface area and pore size distribution (IUPAC technical report). Pure Appl Chem 2015;87(9-10):1051–69. https://doi.org/10.1515/pac-2014-1117.
[46] Giles CH, Smith D, Huitson A. A general treatment and classification of the solute adsorption isotherm. I: Theoretical. J Colloid Interface Sci 1974;47:755–65. https://doi.org/10.1016/0021-9797(74)90252-5.
[47] Sing KSW, Everett DH, Haul RAW, Moscou L, Pierotti RA, Rouquerol J, et al. Reporting physisorption data for gas-solid systems with special reference to the determination of surface area and porosity. Pure Appl Chem 1985;57:603–19. https://doi.org/10.1351/pac198557040603.
[48] Lin L, Lei Z, Wang L, Liu X, Zhang Y, Wan C, et al. Adsorption mechanisms of high–levels of ammonium onto natural and NaCl–modified zeolites. Sep Purif Technol 2013;103:15–20. https://doi.org/10.1016/J.SEPPUR.2012.10.005.
[49] Berkessa YW, Mereta ST, Feyisa FF. Simultaneous removal of nitrate and phosphate from wastewater using solid waste from factory. ApWS 2019;9(2):28. https://doi.org/10.1007/S13201–019–0906–Z.
[50] Abukhadra MR, Ali SM, Nasr EA, Mahmoud HAA, Awwad EM. Effective sequestration of phosphate and ammonium ions by the bentonite/zeolite Na–P composite as a simple technique to control the eutrophication phenomenon: realistic studies. ACS Omega 2020;5(24):14656–68. https://doi.org/10.1021/ACSOMEGA.0C01399.